Land Cover Change Detection using Satellite Remote Sensing For Damaged Area Mapping

Yuta Ikezawa*, Masataka TAKAGI**

Department of Infrastructure System Engineering

Kochi University of Technology

Tosayamada, Kochi, Japan

*E-mail: 155073h@gs.kochi-tech.ac.jp

**E-mail: takagi.masataka@kochi-tech.ac.jp

ABSTRACT: Recently, the large scale disasters are occurred frequently. Therefore, the disaster monitoring is very important. The damaged area mapping using satellite image was tried based on land cover classification map it. When satellite imagery can be simulated based on the mechanism of reflectivity from an actual object, the reliable land cover classification will be done.

For the simulation, Light source, Spectral Reflectance and Digital Surface Model should be decided. The spectrum of solar radiation was generated by SMARTS_295 software. In this study, seven categories were selected as land cover classification items which are needle leaf tree, broad leaf tree, grass land, bright bare land, dark bare land, residential area and water body. The spectral reflectances of the objects were measured by a spectroradiometer which produced by OCEAN OPTICS USB4000. Digital surface model was made by combining the terrain elevation model and simple 3D model of land cover. In this study, the 3D model is called object model. The simulation results of seven categories are compared with satellite data. The nearest category is assign to classified land cover.

On March 11 2011, huge earthquake was occurred in the Tohoku, Japan. The tsunami destroyed a lot of houses and damaged by flood. The detection of the damaged area was tried using this classification method. The result showed the flood damaged area was $20600m^2$ in test area 1 and $901800m^2$ in test area 2. Moreover the damaged area of the residential quarter was $1151800m^2$ in test area 1 and $889600m^2$ in test area 2. These results were obtained from only satellite data. The results should be verified using aerial photograph and field survey.

KEYWORDS: Satellite Remote Sensing, Land cover classification, Simulation of Satellite Image

1. INTRODUCTION

Recently, the large scale disasters are occurred frequently. Therefore, the disaster monitoring is very important. Figure 1.1 shows aerial photograph of devastation by the large-scale earthquake that occurred in Tohoku, Japan on 11 March 2011. The region was damaged by the tsunami. To recover disaster area, damaged area mapping is required. When automated mapping is developed, the method will be very efficient. Now, we can use aerial photograph and satellite imagery as data source for damaged area mapping.

After the earthquake disaster | Before the earthquake disaster

Figure1.1: Land cover change using Aerial photograph

Table1.1 shows comparison between aerial photograph and satellite imagery. The aerial photograph has high resolution. However, the swath the photograph is so narrow that monitoring whole area is difficult. On the other hand, satellite imagery can take wide swath. Then wide area mapping is possible. For example, AVNIR-2 sensor on satellite ALOS (Advanced Land Observing Satellite) observes with 70km swath. Satellite sensor can also observe visible light and the near-infrared radiation. Totally four spectral bands are observed. Figure1.2 shows the sample image of the AVNIR-2 sensor. The sample image is called false color image (RGB was assigned to Band 4, 3, 2). In this imagery, vegetated area is colored by red. Because, vegetation is reflected very well in near infra-red band. Moreover, the cost of satellite imagery is very low comparing with the aerial photograph. Therefore, the damage area mapping using satellite imagery has some advantages.

The purpose of the present study will make mapping damage area by land cover classification using the satellite image. Methodology of land cover classification will be established by simulation of satellite imagery.

Table1.1: Comparison between Aerial Photograph and Satellite Imagery

1 US dollar is 80 yen

	Aerial photograph (1/20,000)	Satellite Imagery (ALOS AVNIR-2)
Resolution	0.5 m/pixel	10 m/pixel
Width of observation	2 km	70 km
Cost	52.5 \$/km^2	0.06 \$/km^2
Number of Bands	3	4
Wavelength	R G B	Band 1: 420 to 500 nm Band 2: 520 to 600 nm Band 3: 610 to 690 nm Band 4: 760 to 890 nm
Number of Detectors	—	7000/band
Pointing Angle	—	-44 to +44 degree
Bit Length	—	8bits
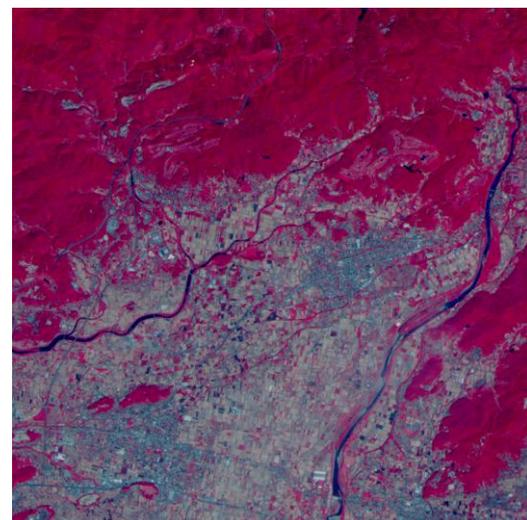
Figure1.2: Sample of AVNIR2 Image

2. METHODOLOGY OF LAND COVER CLASSIFICATION USING SATELLITE REMOTE SENSING

The existing method of land cover classification is

based on operation of spectral band data or statistic method. However, these methods are not based on mechanism of reflectance from actual objects of land cover. Therefore, it is difficult to obtain reliable result. When satellite imagery can be simulated based on the mechanism of reflectivity from an actual object, the reliable method for land cover classification will be developed.

2.1 Simulation of AVNIR-2 Imagery

Figure2.1 shows the general idea of the simulation.
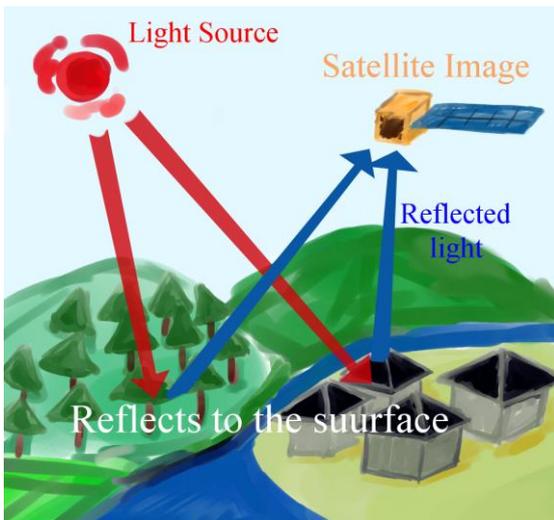
Figure2.1: General Idea of Simulation

Light from the sun is radiated to the ground, and the light is reflected depending on topographic features and characteristics of spectral reflectance on the ground. And the satellite observes the reflected light. Figure2.2 shows flow chart of the simulation of satellite data. For the simulation, Light source, Spectral Reflectance and Digital Surface Model should be decided.
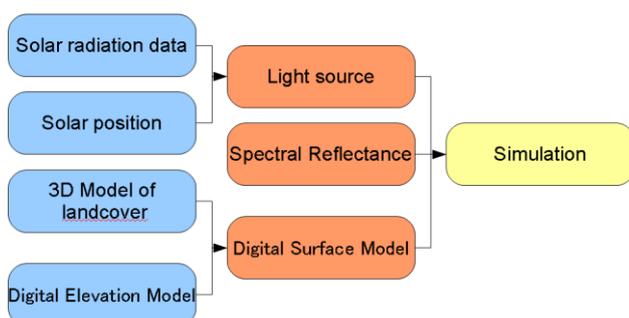
Figure2.2: Flow of simulation

2.1.1 Light source

The spectrum of solar radiation was generated by SMARTS_295 software. The software is produced by NATIONAL RENEWABLE ENERGY LABORATORY. Table2.1 shows input parameters for SMARTS_295. The Figure2.3 shows generated spectrum of solar radiation.

Table2.1: Setting parameter in SMARTS_295

Parameters	Setting condition
Site pressore	1013.250 mb
Atmosphere	Mid Latitude Summer
Ozone	Typical Reference Atmosphere
Gaseous Absorption and Pollution	Typical Reference Atmosphere
CO2 Mixing Ratio	390 ppmv
Aerosol Model	Shettle & Fenn Model
Solar Constant	1366.10W/m^2
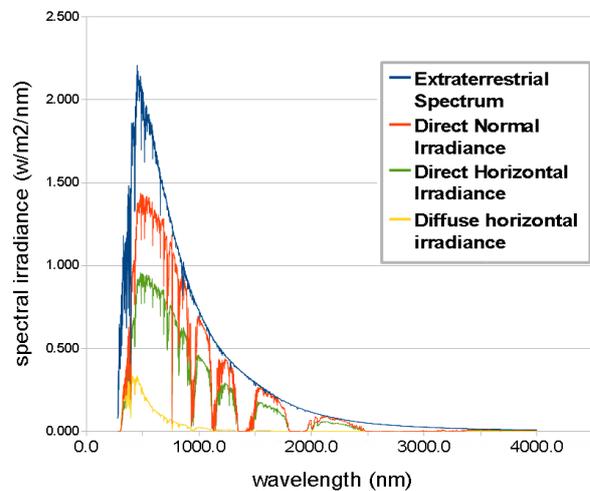
Figure2.3: Solar radiation spectrum

More over, the condition of Light source is changed by the position of the sun. Then the position of the sun was used in the time of satellite data acquisition.

2.1.2 Spectral reflectance

In this study, seven categories were selected as land cover classification items which are needle leaf tree,

broad leaf tree, grass land, bright bare land, dark bare land, residential area and water body. The spectral reflectances of the objects were measured by a spectroradiometer which produced by OCEAN OPTICS USB4000. This spectroradiometer can measure 480 to 900nm in wave length. This measurement was carried out using Halogen Lamp in the dark room. Figure2.4 shows the spectral reflectivity of each object. The spectral reflectivity of each band in AVNIR-2 Sensor was derived by average calculation. In the case of band1, average of reflectivity was calculated from 480 to 500nm. The spectral reflectivity of each object in each band is shown in Table2.2.
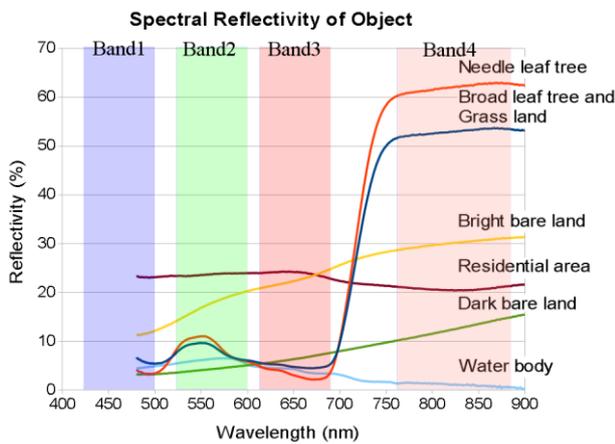
Figure2.4: Spectral reflectivity of each object

Table2.2: Spectral Reflectance in classification category

	Band1	Band2	Band3	Band4
Needle leaf tree	0.0345	0.0890	0.0329	0.6198
Broad leaf tree	0.0541	0.0814	0.0494	0.5291
Bright bare land	0.0321	0.0428	0.0639	0.1260
Dark bare land	0.1188	0.1751	0.2251	0.3012
Grass land	0.0541	0.0814	0.0494	0.5291
Residential area	0.2309	0.2367	0.2388	0.2078
Water body	0.0466	0.0605	0.0398	0.0107

2.1.3 Digital surface model

Digital surface model was made by combining the terrain elevation model and simple 3D model of land cover. In this study, the 3D model is called object model. Figure2.5 shows generation method of digital surface model.
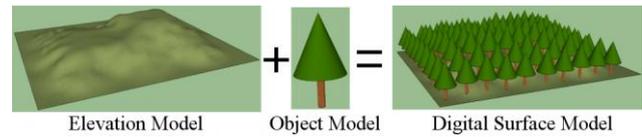
Figure2.5 Generation Method of Digital Surface Model

	Needle leaf tree	Broad leaf tree	Residential area	Grass land	Bright bare land	Dark bare land	Water body
	Cone	Hemisphere	box	Geographical features			
Shape	4m	6m	8m				

Figure2.6: Object model in each category

Terrain elevation model was used 10m grid dataset which are produced by Geographical Survey Institute, Japan.　In this study, Three object models were prepared, which are needle leaf tree, broad leaf tree and residential area. Other Four object models were assumed flat, which are grass land, bright bare land, dark bare land, and the water body. Figure 2.6 shows each shape of each object model. The generated surface model was converted to 1m grid dataset which is called digital surface model.

2.1.4 Simulation Method

The shading and the shadow were calculated using the digital surface model. Eq. (2.1) was used to calculate the shading on the target point.

$$L = L_d + L_r + L_c \qquad \text{Eq. (2.1)}$$

L means the brightness of the object, which is simulation result. L_d, L_r, and L_c means scattered brightness of light source, reflection brightness of light source, and surrounding scattered brightness.

L_d, L_r, and L_c can be calculated by Eq. (2.2), Eq. (2.3) and Eq. (2.4).

$$L_d = R_d L_{in}\cos\theta_i \qquad \text{Eq. (2.2)}$$

L_{in}: Direct normal irradiance

R_d: Diffuse reflection coefficient (0~1)

$$L_r = L_{in}\omega(\theta_i)\cos\gamma \qquad \text{Eq. (2.3)}$$

$\omega(\theta_i)$: Reflectivity

γ: Angle between view point and reflectance

$$L_c = L_d R_d \qquad \text{Eq. (2.4)}$$

L_d: Diffuse horizon irradiance

The Figure2.7 shows situation of position of light source, view point on the target point. The value of Direct normal irradiance and Diffuse horizon irradiance was calculated by SMARTS_295. If the target point was covered by shadow, only L_c was applied directly.
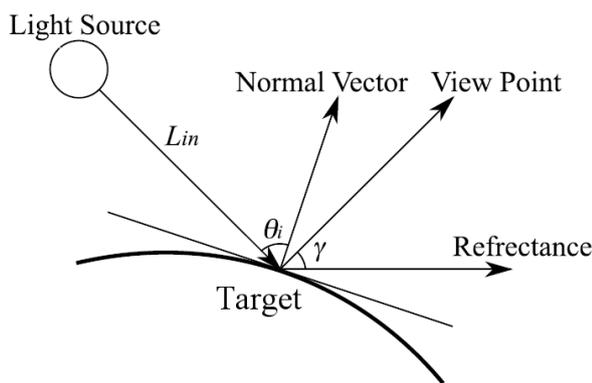
Fgure2.7: Position of light source, view point, and object on a Target point

2.2 Calibration of simulation result

The unit of the simulated value is not same with the unit of actual satellite data. Therefore, a calibration should be carried out. The regression analysis was applied for the calibration. Typical area in each land cover category on the used satellite imagery was used as training data for the regression analysis.

2.3 Classification Method using Simulated Date

The image coordinates of the satellite image are converted into the ground coordinates using the geometric model. In this study Direct Linear Transformation was used as geometric model. The geometric model was established using ground control points. And the simulation of each classification category is executed using digital surface model. Finally, the simulation results of seven categories are compared with satellite data. The nearest category is assign to classified land cover.

3. CASE STUDY IN THOUKU AREA JAPAN

On March 11 2011, huge earthquake was occurred in the Tohoku, Japan. The tsunami destroyed a lot of houses and damaged by flood. The detection of the damaged area was tried using this classification method. As the test area, Ishinomaki City Miyagi Prefecture was selected. Figure3.1 shows the location of the test area.
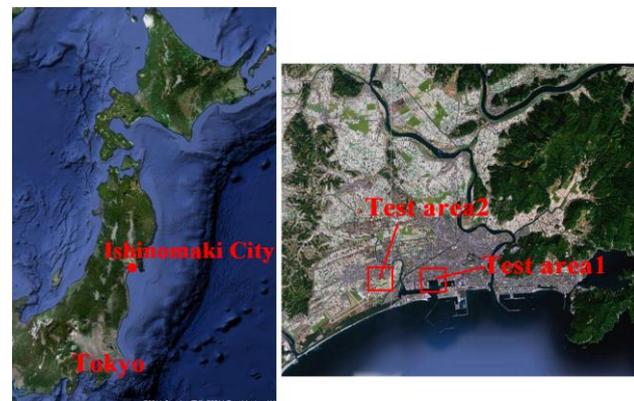
Figure3.1: Location of test area

Test area 1 is near the Ishinomaki port. Test area 2 is around Sada River. Figure3.2 shows the satellite image of the test area 1 before the earthquake and after the earthquake. Figure3.3 shows the satellite image of the test area 2 before the earthquake and after the earthquake.
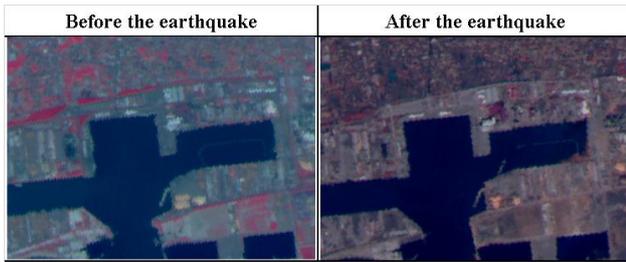
Figure3.2: Satellite image of test area 1
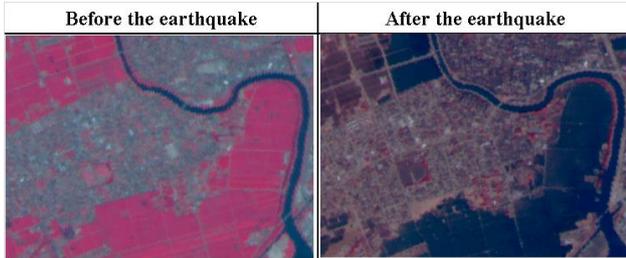
Figure3.3: Satellite image of test area 2

AVNIR-2 image of before the disaster was observed in 8 August 2010. And the AVNIR-2 image of after the disaster was observed in 19 March 2011.

The calibration of the simulation result was carried out. Table3.1 and Table3.2 shows correlation coefficient with the simulation data and satellite imagery in each category. In Table3.1 Correlation coefficients of needle leaf tree and broad leaf tree showed very low. Because, relationship between 3D object model and sun elevation might be influenced. In the both test area, there are few forest. Then, this classification method was applied.

Table3.1: Correlation coefficient of simulation data before disaster

	Band1	Band2	Band3	Band4
Needle leaf tree	0.0742	0.1783	0.0000	0.5480
Broad leaf tree	0.3181	0.3663	0.2624	0.4542
Bright bare land	0.3254	0.5191	0.5488	0.3734
Dark bare land	0.8347	0.7900	0.6580	0.4400
Grass land	0.7549	0.8234	0.6599	0.6293
Residential area	0.3576	0.1109	0.1780	0.5883

Table3.2: Correlation coefficient of simulation data after disaster

	Band1	Band2	Band3	Band4
Needle leaf tree	0.3373	0.5484	0.4447	0.7854
Broad leaf tree	0.4673	0.4972	0.3901	0.7721
Bright bare land	0.7843	0.8793	0.8898	0.8672
Dark bare land	0.8361	0.5316	0.7633	0.2530
Grass land	0.1752	0.0500	0.1175	0.7369
Residential area	0.3793	0.0964	0.3051	0.6361

Land cover classification was carried out using calibrated simulation data. Figure3.4 shows legend of the seven categories. Figure3.5 shows the classification of the test area 1 before the earthquake and after the earthquake. Figure3.6 shows the classification map of the test area 2 before the earthquake and after the earthquake.

Figure3.4: Legend of the classification category
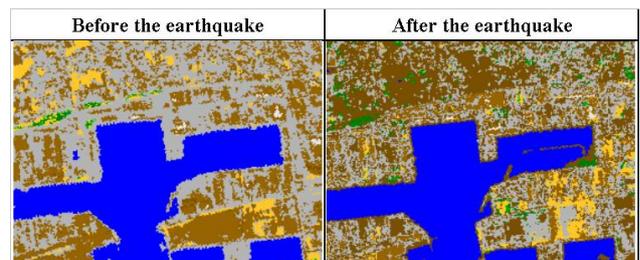
Figure3.5: Classification map in test area 1

| Before the earthquake | After the earthquake |
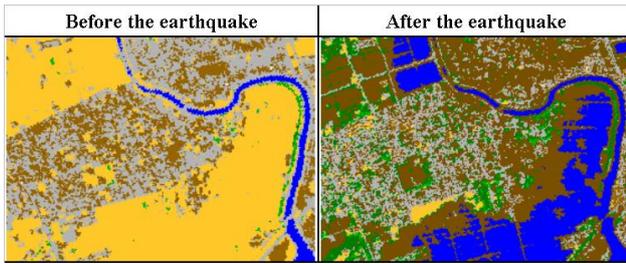
Figure3.6: Classification map in test area 2

The classification result before the disaster and after the disaster was analyzed by cross tabulation. The cross tabulation in test area 1 is shown in Table3.3.

Table3.3: Cross tabulation table in test area 1 (%)

		After the disaster				
		Water body	Forest	Grass land	Bare land	Residential area
Before the disaster	Water	92.7	0.7	0.0	6.2	0.5
	Forest	0.0	31.8	0.0	52.9	15.3
	Grass land	0.4	14.4	13.4	47.1	24.8
	Bare land	0.1	1.8	7.3	51.8	39.0
	Residential area	0.9	3.0	4.3	54.2	37.6

Test area 1 had changed a lot of residential area to the bare land after the disaster. 54.2% of residential area were destroyed.

The cross tabulation of test area 2 is shown in Table3.4

Table3.4: Cross tabulation table in test area 2 (%)

		After the disaster				
		Water body	Forest	Grass land	Bare land	Resident ial area
Before the disaster	Water	84.3	0.0	0.0	15.6	0.1
	Forest	10.8	52.1	0.0	36.4	0.7
	Grass land	33.6	14.0	2.7	44.0	5.6
	Bare land	0.0	7.6	3.1	47.3	41.9
	Residential area	2.3	12.7	2.1	53.0	29.9

In the test area 2, a lot of grass lands were changed to the water body after the disaster. It seems these areas are damaged by flood. And also, a lot of residential areas were changed to bare land. 33.6% of grass land were flooded, 53% of residential area were destroyed.

The damaged areas were mapped according to result of cross tabulation (Figure3.7). Moreover, the total damaged area was calculated by counting pixels on damaged map. Table3.5 shows the damaged area of the calculated test area. In the both test area, over 30% areas were damaged by tsunami.

| Test area 1 | Test area 2 |

🟥 Damage of residential area
🟦 Damage of flood
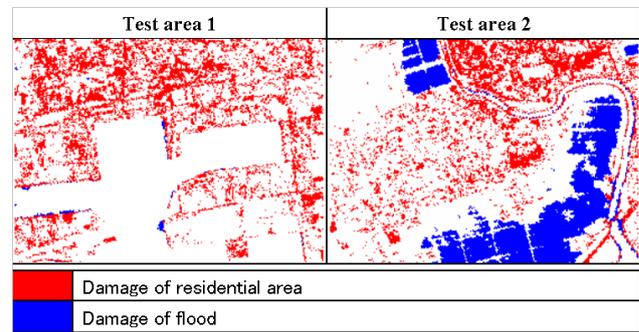
Figure3.7: Damaged area map in test area

Table3.5: Damaged area in test area

	Damaged area of Residential area		Damaged area of flood	
Test area1	1,151,800m^2	29.5 %	20,600 m^2	0.5%
Test area2	889,600m^2	16.2%	901,800 m^2	16.4%

4. CONCLUSIONS

Method of simulation of satellite data was established. The land cover classification using satellite image based on simulated data was successfully finished. And the detection of the damaged area using the classification map was tried. The result showed the flood damaged area was 20600m^2 in test area 1 and 901800m^2 in test area 2. Moreover the damaged area of the residential quarter was 1151800m^2 in test area 1 and 889600m^2 in test

area 2. These results were obtained from only satellite data. The results should be verified using aerial photograph and field survey.

REFERENCES

Y. Kikuchi, M. Takagi, Shadow extraction and urban classification from ASTER image using mixed pixel analysis, Takagi Laboratory, Kochi University of Technology, 2003

S. Aksoy, K. Koperski, C. Tusk, and G. Marchisio, Land Cover Classification with Multi-sensor Fusion of Partly Missing Data, *PHOTOGRAMMETRIC ENGINEERING & REMOTE SENSING*, Vol75, No5, pp577-592,2009

H.Bagan, Y. Ymagata, Improved Subspace Classification Method for Multispectral Remote Sensing Image Classification, *PHOTOGRAMMETRIC ENGINEERING & REMOTE SENSING*, Vol76,No11,pp.1239-1251,2010